Zero-cooling energy thermoelectric system by phase change material heat sink integrated with porous copper foam

Rezaniakolaei, Alireza; Yousefi, Esmaeil ; Abbas Nejad, Ali

Published in:
Journal of Energy Storage

DOI (link to publication from Publisher):
10.1016/j.est.2022.106507

Publication date:
2023

Document Version
Publisher's PDF, also known as Version of record

Journal of Energy Storage 59 (2023) 106507

Contents lists available at ScienceDirect

Journal of Energy Storage

journal homepage: www.elsevier.com/locate/est

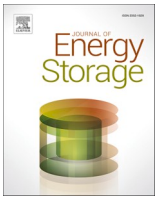

Research papers

Zero-cooling energy thermoelectric system by phase change material heat sink integrated with porous copper foam

Alireza Rezania [a,*], Esmaeil Yousefi [b], Ali Abbas Nejad [b]

[a] AAU Energy, Aalborg University, Pontoppidanstræde 111, Aalborg DK-9220, Denmark
[b] Faculty of Mechanical Engineering, Shahrood University of Technology, Shahrood, Iran

ARTICLE INFO

Keywords:
Thermoelectric generator
Dynamic heat loads
Phase change material
Porous metal foam
Zero-cooling energy

ABSTRACT

Active cooling of thermoelectric generators (TEGs) by fans or water pumps imposes cooling energy reducing net power generation in TEG systems. This study aims to make zero-cooling energy TEG systems by integration of low temperature phase change material (PCM) and porous copper foam on cold side of the TEG. In this design, air fan is eliminated. To study the proposed system under transient heat input, the TEG system was exposed to continues and dynamic heat flows. Results of this study show that, the proposed fanless heat sink is an effective and alternative cooling solution for TEG systems. Utilization of the copper foam in the PCM not only reduced cold side temperature of the TEG by 11.3 %, but it also prevents hot side of the TEG from overheating. With this cooling technique, output power of the TEG increased 53.5 % compared to conventional TEG systems operating with fan. The results of this study provide a guideline for design of self-sufficient and autonomous TEG systems with zero-cooling energy used for energy harvesting for sensors and actuators under dynamic heat sources.

1. Introduction

Thermoelectric generators (TEGs) work based on the Seebeck effect to convert heat directly into electricity with no moving parts or complicated structure. Although, TEGs have low energy conversion efficiency [1,2], proper cooling system and thermal management mechanisms can increase temperature difference across the TEG, and enhance the efficiency [3,4]. Efficient design of heat sink is one of the critical factors in performance of TEG systems when hot side of the TEG is exposed to high-amplitude temperature variations and there is risk for overheating and system damage [5]. Nevertheless, a high performance cooling system imposes a cost for higher power generation by a TEG [6].

One technique for stabilizing temperature fluctuations on TEG surfaces under transient thermal conditions is utilization of phase change material (PCM) [7] for its high thermal energy storage capacity as heat of fusion [8,9]. In thermoelectric systems, PCM can be used on the cold side of a TEG as a heat sink [10]. Selvam et al. [11] modelled thermal effect of PCM as heat sink for thermal management of a thermoelectric system, where the system performance enhanced in term of power generation. Ahmadi et al. [12] also reported higher output voltage in TEGs using PCMs on cold side of the TEGs in an experimental study. They, furthermore, investigated critical parameters in a hybrid TEG-PCM system and found that, thermal resistance of the heat sink have significant effect on the TEG's output power [13]. In an experimental study, Muthu et al. [14] improved conversion efficiency of hybrid solar parabolic dish-TEG systems by employing PCM-based heat sink.

PCM-based heat sinks offer advancing thermoelectric energy harvesting with more effective thermal management for wireless sensor applications. Bertacchini et al. [15] utilized PCM to supply continues condition monitoring of wireless sensor systems placed in a vehicle engine section. The PCM-based heat sink proposed by them enhanced cooling performance in the system under steady state and transient thermal conditions. Despite high capacity for thermal storage, PCMs have generally low thermal conductivity, which reduces heat conductance from the TEG to the environment ambient. This is a main factor in overheating of the TEG. Amplification of PCM's thermal conductivity is, therefore, a key parameter to control and stabilize temperature of TEGs under transient thermal loads and to provide stable output power [16].

Novel concepts have been suggested to enhance heat storage and heat transfer performances of PCMs. Biomimetic red blood cell shaped PCMs are compared to traditional spherical shape capsules using characterization of external flows around the capsules [17]. The flow attack angel was optimized based on minimizing drag force and maximizing Nusselt number. Furthermore, biomimetically calabash-inspired shapes [18] and oval structure [19] PCMs are studied for investigation of

* Corresponding author.
E-mail address: alr@energy.aau.dk (A. Rezania).

https://doi.org/10.1016/j.est.2022.106507
Received 28 June 2022; Received in revised form 14 December 2022; Accepted 20 December 2022
Available online 27 December 2022

Nomenclature

C_p	specific heat capacity (J $kg^{-1}K^{-1}$)
C_{th}	equivalent thermal capacitance (JK^{-1})
f	volume fraction
h	height (m)
I	current (A)
k	thermal conductivity (W $m^{-1}K^{-1}$)
L	latent heat capacity (J kg^{-1})
l	length (m)
P	power (W)
Q	heat transfer (W)
R_{in}	internal resistance (Ω)
R_L	external load (Ω)
R_{th}	thermal resistance (KW^{-1})
S	Seebeck coefficient (VK^{-1})
T	temperature (°C, K)
t	time (s)
V	voltage (V)
w	width (m)

Greek letters

α	Thermal diffusion (m^2s^{-1})
ΔT	temperature range over which the PCM melts (K)
ε	porosity
ρ	density (kg m^{-3})

Subscripts

app	apparent
Al	aluminum
c	cold
Foam	metal foam
h	hot
l	liquid state of PCM
m	metal
max	maximum
melt	melting point
PCM	phase change material
pm	porous medium
s	solid state of PCM
TEG	thermoelectric generator

overall thermal performance of these layouts.

Heat transfer enhancement of PCMs integrated with porous metal foams has been investigated in several studies for thermal energy storage [20]. Porous metal foams are suitable materials for enhancing thermal conductivity of PCMs [21,22]. These materials have been studied in many thermal applications such as heat exchangers, medicine, and solar collectors because of their light-weight, high surface density and compact size [23]. Ali [24] showed that, hybrid PCM and metal foam heat sink can obstruct rapid upsurge of temperature under dynamic heat loads with inconsiderable cost.

Utilization of metal foams in small-scale PCM storage packs are proposed to enhance performance of thermoelectric systems [25]. Wang et al., [26] developed electrically insulating PCMs for implementation on cold side of TEGs, for superior power output of TEGs. In order to enhance heat transfer rate in PCMs, Borhani et al. [27] conducted a numerical study with adding copper foams to PCMs on both sides of a TEG module (paraffin RT35 on the cold side and paraffin RT69 on the hot side), which resulted higher thermoelectric performance at lower metal porosities. Nithy et al. [28] applied heat exchangers made of porous metal foams on host side of TEGs leading to higher heat recovery from car's exhaust pipe. Madroga [29] integrated aluminum porous foam with PCM used for thermoelectric systems in the fuselage of an aircraft. They observed, the metal foam is a main factor for achieving a suitable temperature difference across the TEG and higher output power during flights. In another study [30], he introduced a model for hybrid TEG-PCM modules integrated with aluminum foam to transform ambient thermal fluctuations into electrical energy. Combination of PCMs and porous copper foam was employed as an effective heat sink by Duan [31] for cooling of concentrated photovoltaic systems. In his study, embedding the metal foam in the PCM significantly enhanced the cooling effect and increased the electrical efficiency of the proposed system compared to a system operating with pure PCM as heat sink.

Providing suitable temperature on cold side of TEGs is a great challenge in efficient thermoelectric systems. Using powerful cooling fans for effective cooling, on the other hand requires high electrical energy, which decreases thermoelectric net power generation. The net power in self-cooling TEG systems is investigated and discussed in detail in an experimental study by Mohammadnia et al. [32]. They studied effect of electrical input power of cooling fans, supplied by the TEG system, on performance of thermoelectric energy harvesting system and showed that, feasibility of utilization of the cooling fans in a self-cooling TEG system is strongly related to its thermal boundary conditions. At low temperatures, utilization of self-cooling system is not efficient because the power generation is smaller than electrical power required for the electrical fan. On the other hand, removing the active cooling fan can damage the TEG due to overheating and temperature fluctuations under dynamic heat loads. Therefore, exploring alternative cooling strategy is critical.

Passive cooling approaches can offer thermoelectric systems with zero-cooling energy. Wang et al. [33,34] suggested radiative cooling based on ultra-cold outer space to deliver all-day passive thermoelectric power generation. Moreover, as shown in [7], passive cooling with integration of natural convection heat transfer and PCM has potential to remove cooling fan from TEG systems toward zero-cooling energy consumption under transient heat loads. Nevertheless, PCMs have low thermal conductivity causing overheating condition and temperature inflation on the TEG's cold side and decreasing conversion efficiency of the system. This study aims to introduce fanless and zero-cooling energy heat sink for thermoelectric energy harvesting systems operating under dynamic heat sources. This heat sink integrates high heat capacity of PCM with high thermal conductivity of porous metal foam to provide effective cooling and to eliminate electric power consumption for cooling of the system.

This experimental study, therefore, investigates effectiveness of copper metal foam to increase thermal conductivity in the PCM in a hybrid heat sink. Despite of bigger cooling system size, this study intents improving thermal management of TEGs as well as enhancing thermoelectric output power under dynamic thermal boundary conditions by replacing conventional cooling fans with the hybrid design of PCM and metal foam heat sinks. Since the time-dependent heat transfer through the thermoelectric energy harvester system is a function of thermal conductivity and heat capacity of the heat sink, heat transfer across the energy harvester system is carefully explored.

In order to show impact of the porous metal foam on heat transfer through the PCM, result of the proposed hybrid heat sink (PCM—Cu) with zero-cooling energy is compared with a conventional TEG system (with fan), a fanless system (no fan), and a TEG system with PCM but without the copper foam (PCM-only). Accordingly, in the next section, equivalent RC network of the system consisting of geometry and thermal properties of the hybrid heat sink is presented and used to evaluate heat transfer mechanism under continues and fluctuating heat fluxes. To explain mechanism of the zero-cooling energy heat sink, its design concept and relevant governing equations are presented. Section 3 describes the experimental setup, theoretical calculations, and test

procedure in this study. Results of this study are discussed in Section 4 followed by conclusions.

2. Equivalent RC design and governing equations

Fig. 1 shows the RC network model of the system and the governing equations to clarify concept of heat transfer mechanism on the cold side of the TEG, where R and C are the thermal resistance and capacitance, respectively, defined as [35]:

$$R_{th} = \frac{h}{w\, l\, k} \tag{1}$$

$$C_{th} = h\, w\, l\, \rho\, C_{app} \tag{2}$$

In Eqs. (1) and (2), the parameters of h, w and l are the thickness, width, and length of the RC network components, respectively. The terms of k and ρ represent thermal conductivity and density for each element, and $C_{app}$is the apparent heat capacity of the PCM expressed as:

$$C_{app} = \begin{cases} C_p & , \quad T \le T_{melt} \\ C_p + \dfrac{L}{\Delta T} & , \quad T_{melt} < T < T_{melt} + \Delta T \\ C_p & , \quad T \ge T_{melt} + \Delta T \end{cases} \tag{3}$$

where L and ΔT are latent heat of the PCM and range of melting temperature.

Before adding the foam to the PCM in the box, $R_{th,\,AB}$ and $C_{th,\,AB}$ from A to B can be expressed as follow:

$$\frac{1}{R_{th,AB}} = \frac{1}{R_{th,Al}} + \frac{1}{R_{th,PCM}} \tag{4}$$

$$C_{th,AB} = C_{th,Al} + C_{th,PCM} \tag{5}$$

With the porous foam added to the PCM, Eqs. (4) and (5) become as follow:

$$\frac{1}{R_{th,AB}} = \frac{1}{R_{th,Al}} + \frac{1}{R_{th,PCM}} + \frac{1}{R_{th,Foam}} \tag{6}$$

$$C_{th,AB} = C_{th,Al} + C_{th,PCM} + C_{th,Foam} \tag{7}$$

Eqs. (6) and (7) confirm that the foam reduces the thermal resistance of the PCM in the system and increases its heat capacity. The thermal resistance and heat capacitance of the porous medium, R_{pm} and $C_{th,\,pm}$, can be expressed as follow:

$$\frac{1}{R_{th,pm}} = \frac{1}{R_{th,PCM}} + \frac{1}{R_{th,Foam}} \tag{8}$$

$$C_{th,pm} = C_{th,PCM} + C_{th,Foam} \tag{9}$$

The governing equations can be expanded by substitution of Eqs. (8) and (9) into Eqs. (6) and (7):

$$\frac{1}{R_{th,AB}} = \frac{1}{R_{th,Al}} + \frac{1}{R_{th,pm}} \tag{10}$$

$$C_{th,AB} = C_{th,Al} + C_{th,pm} \tag{11}$$

where $R_{th,\,pm}$ and $C_{th,\,pm}$ are defined as follow:

$$R_{th,pm} = \frac{h}{w\, l\, k_{pm}} \tag{12}$$

$$C_{th,pm} = h\, w\, l\, \overline{\rho\, C} \tag{13}$$

The term of porous medium conductivity, k_{pm}, can be expressed as [36] follows:

$$k_{pm} = (1-\varepsilon)\, k_m + \varepsilon\, k_{PCM} \tag{14}$$

where k_m is thermal conductivity of the foam material. Also, thermal conductivity of the PCM, k_{PCM}, is defined as follows:

$$k_{PCM} = f_l k_l + (1-f_l)\, k_s \tag{15}$$

Mean thermal capacitance of the porous medium, $\overline{\rho\, C}$, in Eq. (13) can be expressed as follows:

$$\overline{\rho\, C} = f_l\, \varepsilon\, \rho\, C_l + (1-f_l)\, \varepsilon\, \rho\, C_s + (1-\varepsilon)\, \rho_m C_m \tag{16}$$

where C_m indicates the specific heat of the foam material, and C_s and C_l are the specific heat of the solid and liquid phases of the PCM, respectively. Moreover, ε is the porosity of the porous matrix, and ρ and ρ_m are density of the PCM and porous matrix, respectively. The term of f_l is the volume fraction of the PCM in the liquid phase as follows [37]:

$$f_l = \begin{cases} 0 & , \quad T \le T_s \\ 1 & , \quad T \ge T_l \\ \dfrac{T - T_s}{T_l - T_s}, & T_s < T < T_l \end{cases} \tag{17}$$

Thermal boundary conditions, imposed on the TEG by the heat source and PCM box, determine temperature on the hot and cold sides of the TEG. Eqs. (18) and (19) show output voltage and power in the TEG [38].

$$V = I_{TEG} R_L \tag{18}$$

$$P = I_{TEG} V \tag{19}$$

The terms of I_{TEG} and R_L are the electrical current and external load connected to the TEG, respectively. The maximum power generation in a TEG can be achieved when the external load resistance is equal to TEG's

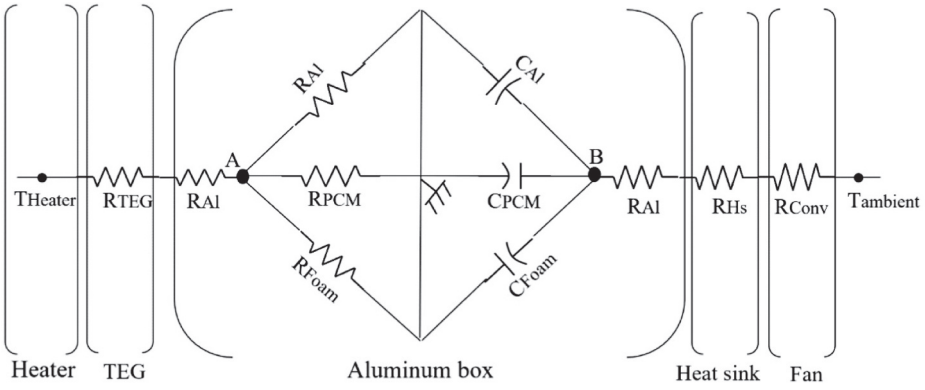

Fig. 1. RC network model of thermoelectric system in this study.

internal electrical resistance (R_{in}) [39]. Thus:

$$P_{max} = \frac{S^2(T_h - T_c)^2}{4R_{in}} \quad (20)$$

where S is the Seebeck coefficient and T_h and T_c are the temperatures on the hot and cold sides of the TEG, respectively. Cooling power required on the cold side of the TEG can be a critical factor in net power in a TEG system. With significant cooling power, the net power in the TEG system is minor and the TEG system becomes impractical. Net power in a TEG system can be defined as follows [40]:

$$P_{net} = P_{max} - P_{cooling} \quad (21)$$

3. Experimental setup, theoretical calculations, and test procedure

This section describes the experimental setup, theoretical calculations of thermal properties of the system's components, and methods used to conduct the tests in this study.

3.1. Experimental setup

In this study a thermoelectric module (SP1848-271455A), with dimensions of 40 mm × 40 mm × 4 mm, was used as the energy harvester. Two ceramic heat plates with dimensions of 15 mm × 70 mm × 1.5 mm and maximum power and voltage of 210 W and 220 V, respectively,

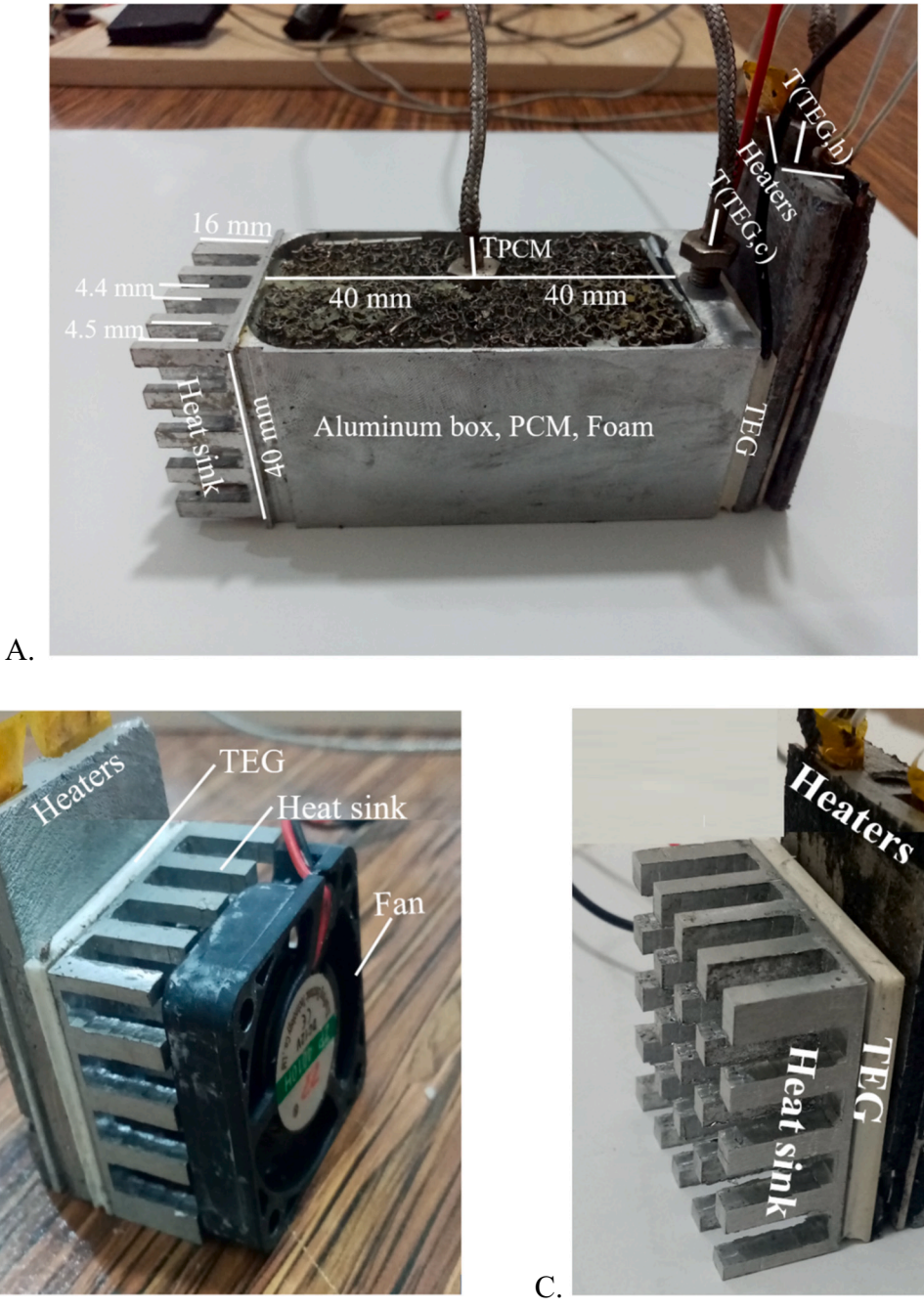

Fig. 2. A: Studied TEG systems with PCM box and copper porous foam, and location of the thermocouples before insulation. B: Conventional TEG system with fan. C: Fanless TEG system without PCM heat sink.

simulated the heat loads. Fig. 2 furthermore shows the TEG systems investigated in this study. In the TEG system with fan, a 12 V DC axial fan (ZhangPeng 4010H) was used. The aluminum heat sink had dimensions of 40 mm × 40 mm × 16 mm with 20 fins each with dimensions of 4.4 mm × 4.4 mm × 15 mm. The PCM storage box, with wall thickness of 0.6 mm, had length and volume of 80 mm and 128.000 mm^3, respectively. The aluminum box was designed to contain the PCM and metal foam to conduct heat from the TEG to the heat sink and environmental ambient. Thermal properties of the PCM and open porous copper foam are specified in Tables 1 and 2, respectively. As shown in Fig. 2A, K-type thermocouples with temperature measurement up to 1250 °C and error of 0.75 % were used in the experiments. To minimize and neglect heat loss, K-Flex insulators with thermal conductivity of 0.036 (W $m^{-1}K^{-1}$) and average thickness of 25 mm was used to insulate the system from the environmental ambient.

3.2. Theoretical calculations

According to the specifications of the studied thermoelectric system, the thermal resistance and heat capacitance of the system elements from A to B in Fig. 1, before adding the copper foam in the PCM, are calculated using Eqs. (1) and (2) and presented in Table 3. Therefore, $R_{th,\ AB}$ and $C_{th,\ AB}$ are calculated using Eqs. (4) and (5) and shown in Table 4.

Moreover, thermal resistance and heat capacitance of the porous medium are calculated using Eqs. (12) and (13) as shown in Table 5. Eqs. (14) and (16) were applied to calculate k_{pm} and $\overline{\rho\ C}$.

Finally, values of $R_{th,\ AB}$ and $C_{th,\ AB}$, after adding the copper foam in the PCM, were calculated according to Eqs. (10) and (11) and presented in Table 6 as follows:

The results in Tables 4 and 6 show the thermal resistance reduced and the heat capacitance increased in the aluminum box after applying the copper foam in the PCM.

3.3. Tests procedure

The tests performed in this study are categorized into four cases to show advantage of using hybrid PCM and metal foam heat sink over conventional cooling methods used for thermoelectric systems. The considered cases are; TEG without the PCM heat sink but with cooling fan (Case#1), fanless system without the PCM heat sink (Case#2), fanless system with PCM but without the metal foam (Case#3; PCM-only), and fanless system where the foam is applied in the PCM heat sink (Case#4; PCM—Cu). Fig. 2 illustrates these thermoelectric systems. Moreover, various of heat loads with different amplitudes and durations are investigated in this study. Table 7 shows characteristics of the applied heat loads.

Fig. 3 illustrates some of the continues and dynamic shape heat loads in this study. In all the tests, the heater was turned off after the TEG's hot side reached 150°C defined as the critical temperature for overheating condition.

The system with the fan, see Fig. 2B, is considered as the basic design for conventional thermoelectric systems. By removing the fan (Fig. 2C), the system was cooled down only via natural convection of air from the heat sink's fins surfaces. Evaluation of the fanless system in Case#2 not only provides a feasibility study of cooling by natural convection for TEG systems under transient heat loads, but the results was used also for comparison with the systems consisted of PCM and metal foam. With porosity of ε= 0.9 for the metal foam, volume of the PCM used in the PCM-Cu system reduced to 115.200 mm^3 as shown in Fig. 2A.

Table 1
Properties of the phase change material [41].

PCM	T_m(°C)	ρ(kg m^{-3})	L(J kg^{-1})	C_p(J $kg^{-1}K^{-1}$)	k_{th}(W $m^{-1}K^{-1}$)
Pure paraffin	36.5	820 (s) 780 (l)	237,000.4	1900 (s) 2200 (l)	0.212 (s) 0.16 (l)

Table 2
Copper foam properties with dimensions of 40 mm × 40 mm × 80 mm and tolerance of ±0.1 mm.

Material	Pores per inches (PPI)	Porosity	C_p(J $kg^{-1}K^{-1}$)	ρ(kg m^{-3})	k_{th} (W $m^{-1}K^{-1}$)
Copper	20	0.90	385	8933	401

For maximum power generation, the external load resistance over the TEG is equal to the TEG's internal resistance [39,42]. Therefore, an external load resistance of 5 Ω was applied over the TEG in all experiments in this study. To verify repetition of the experimental results, each test was conducted three times. Standard deviation of the parameters measured in the tests was calculated as follows [43]:

$$s_x = \left[\frac{1}{n-1}\sum_{i=1}^{n}(x_i - \overline{x})^2\right]^{\frac{1}{2}} \tag{22}$$

where n is number of the measurement. The mean value of x is defined as follows:

$$\overline{x} = \frac{1}{n}\sum_{i=1}^{n} x_i \tag{23}$$

Thus, the experimental uncertainty of the output voltage, and the hot and cold side temperatures of the TEG are calculated 0.1 V, ±1.5°C, ±1°C, respectively.

4. Results and discussion

This section begins with discussion on impact of conventional cooling system with fan on performance of the TEG system. Next, adding the PCM to the fanless systems is evaluated to show improvement of the cooling performance with the thermal energy storage module. This represents a zero-cooling energy system but inefficient to protect the TEG from overheating condition. Furthermore, effect of the porous metal foam on heat transfer in the PCM is shown, where the system performance in terms of power generation and protection from overheating is discussed. These evaluations are performed under continues heat loads at environmental ambient temperature. The thermoelectric systems with zero-cooling energy were, furthermore, investigated under periodic heat loads to highlight superior performance of the hybrid cooling technique made with integration of the PCM with the metal foam. Last, energy harvesting improvement of the hybrid cooling technique suggested in this study is compared with the other cases under both continues and periodic heat loads.

4.1. Conventional TEG system with electrical fan versus TEG systems with zero-cooling energy

Fig. 4 shows the TEG's cold and hot sides temperature variation in the conventional TEG system (Case#1) and the fanless system (Case#2) under 5 W electric power imposed by the heater.

The significant effect of the fan to reduce the cold side temperature of the TEG can be seen by comparing the results of the Case#1 and Case#2. With higher heat transfer coefficient on the cold side due to the operating fan, the temperature on the hot side also decreases. The hot side temperature in the Case#1 reached the critical temperature at 150 °C after 750 s, while in the system with the fan the hot side temperature was 117 °C at the same time. It took 1/3 of time for the system in Case#2 to reach the same temperatures as the system with fan, Case#1, at the hot and cold sides of the TEG. Therefore, to make high performance TEG system, proper cooling mechanism is essential. Especially, overheating can be a threat for the TEG under higher heat loads. Removing the fan in conventional TEG systems reduces the temperature difference across the

Table 3
Thermal resistance and heat capacitance of the TEG system elements from A to B in Fig. 1 before adding copper foam in the PCM.

Material	h (mm)	w (mm)	l (mm)	k (W $m^{-1}K^{-1}$)	R_{th} (KW^{-1})	ρ (kg m^{-3})	C_{app} (J $kg^{-1}K^{-1}$)	C_{th} (JK^{-1})
Al	80	0.6	120	235	4.73	2700	897	13.95
PCM (s)	80	40	40	0.212	235.85	820	1900	199.42
PCM (l)	80	40	40	0.16	312.2	780	2200	219.65

Table 4
$R_{th,\ AB}$ and $C_{th,\ AB}$ before adding foam in the PCM.

PCM state	solid	liquid
$R_{th,\ AB}(KW^{-1})$	4.64	4.66
$C_{th,\ AB}(JK^{-1})$	213.37	233.6

TEG and declines the power generation. However, using the cooling fan is associated with cooling power cost. Therefore, alternative but fanless cooling systems are worthy for investigation in small scale TEG systems.

Fig. 5 shows power generation and temperature difference across the TEG at low value of the heat load for all the cases considered in this study. The results show that, using PCM significantly enhanced the temperature difference and power generation in the TEG due to potential of this material in thermal energy storage. Although removing the electrical fan from the heat sink module decreases the heat transfer coefficient on the cold side of the system (RC network model in Fig. 1), adding the PCM and absorbing the heat transferred from the TEG can keep the cold side temperature of the TEG lower than the Case#2. Therefore, as shown in Fig. 6, adding the energy storage in PCM box, with heat capacitance of $C_{th,\ AB}$ (Eq. (5)), makes delay in reaching the critical temperature on the host side of the TEG. In comparison with the system with no fan in Case#2, this improvement is 254 % with $C_{th,\ AB} = 213.37\ JK^{-1}$, see Table 4.

Based on the Eqs. (22) and (23), Table 8 shows summary of the mean value of voltage generation and standard deviation at 1800 s under 5 W heat load.

Fig. 6 shows temperatures variation of the PCM and TEG as well as temperature difference across the TEG in the systems with the PCM-based heat sink. In comparison with the fanless system (Case#2) shown in Fig. 4, the cold and hot sides temperatures of the TEG in the systems with PCM were reduced significantly. Under transient heat loads, while a fraction of the heat transferred to the cold side of the TEG is stored in the PCM, the heat discharged into environment from the heat sink is a small fraction of the heat imposed to the TEG system simultaneously. Therefore, a heat sink without cooling fan and with a lower heat transfer coefficient to the environmental ambient can be capable to keep the system temperature reasonably low. This improvement makes a unique opportunity to introduce TEG systems with zero-cooling energy. Elimination of the active cooling energy shows the significant effect of using the PCM on the cold side of the TEG to enhance net power in TEG systems, see Eq. (21).

4.2. Enhanced performance at high heat loads with PCM-Cu based heat sink

According to Eq. (6), using the metal foam enhances the heat transfer rate in the PCM box and make more effectual heat sink by improving thermal conductivity and rate of thermal storage in the energy storage box. The PCM melting process was completed in the system with PCM-Cu heat sink even under the low heat load before the TEG reached the critical temperature, see $T_{(PCM\_PCM-Cu)}$ in Fig. 6. Maximum power generation in Case#3, with the PCM-only, was, however, higher than the TEG system with PCM-Cu heat sink under low heat loads. Because of the low thermal conductivity of the PCM box, the hot side temperature of the TEG increased rapidly in Case#3 (see Fig. 6) and made higher temperature difference across the TEG as shown in Figs. 5 and 6. Comparing the results in Tables 4 and 6 show that, the metal foam inserted into the PCM box in the Case#4, increased thermal conductance in the storage box 473 %. As result, the TEG in Case#4 did not reach the critical temperature at the low heat load. The enhanced thermal conductance increased heat transfer from the cold side of the TEG to the ambient. Combination of the enhanced thermal conductance and heat capacitance in the storage box in the TEG system with PCM-Cu heat sink

Table 6
$R_{th,\ AB}$ and $C_{th,\ AB}$ with porous medium in the aluminum box.

Material	Copper foam and PCM (s)	Copper foam and PCM (l)
$R_{th,\ AB}(KW^{-1})$	0.98	0.98
$C_{th,\ AB}(JK^{-1})$	237.45	255.65

Table 7
Pattern of used heat fluxes in the tests.

Heat flux pattern	Electric power (W)	Heater on/ off (s)
Continues	5, 10, 15	–
Dynamic	5, 10, 15	150
Dynamic	5, 10	60
Dynamic	5	240

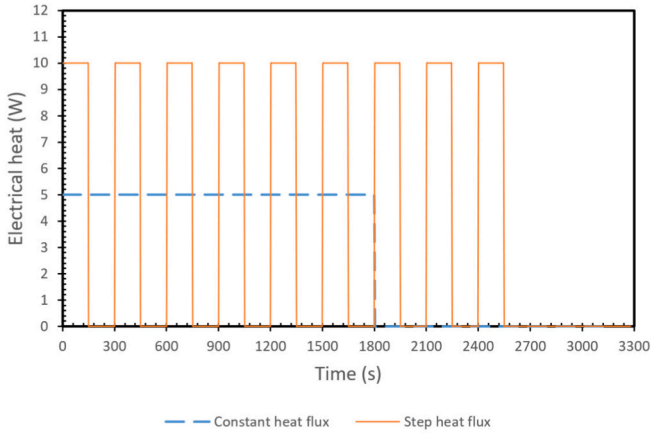

Fig. 3. Electrical heat loads imposed by the heater to the TEG; continues 5 W and dynamic 10 W with on/off duration of 150s.

Table 5
Thermal resistance and heat capacitance of the porous medium in Fig. 1.

Material	h(mm)	w(mm)	l(mm)	k_{pm} (W $m^{-1}K^{-1}$)	R_{pm} (KW^{-1})	$\overline{\rho C}$ ($kJm^{-3}K^{-1}$)	$C_{th,\ pm}$ (JK^{-1})
PCM (s) and foam	80	40	40	40.29	1.241	1746.12	223.5
PCM (l) and foam	80	40	40	40.24	1.242	1888.32	241.7

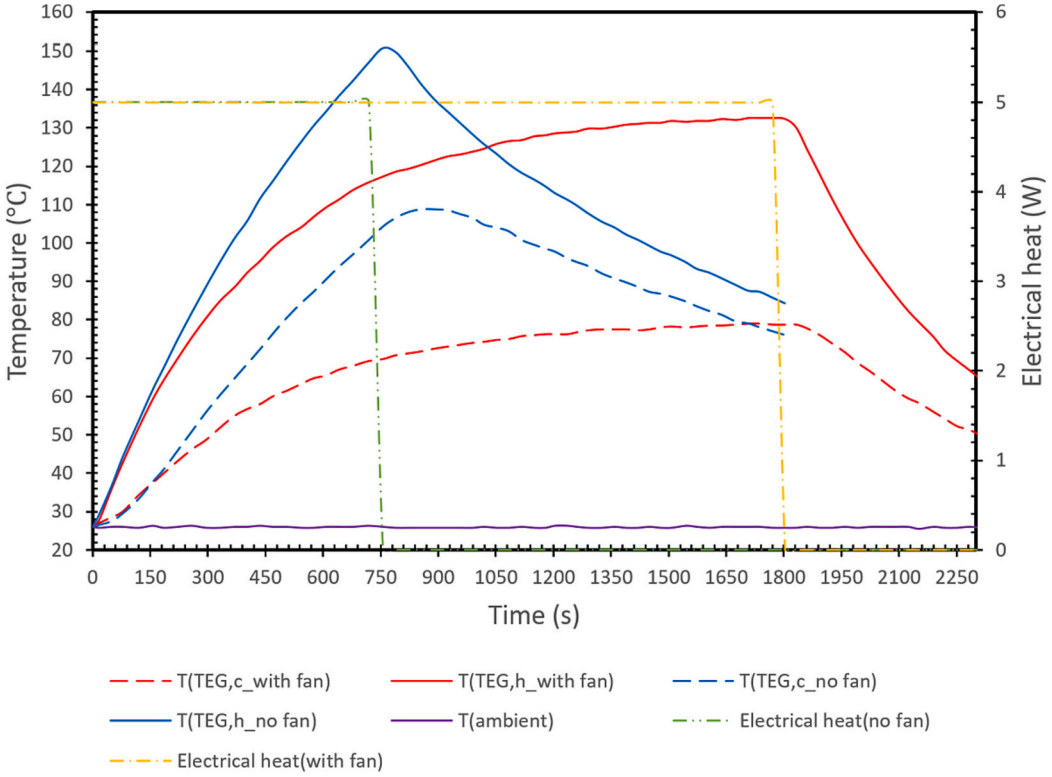

Fig. 4. Hot and cold sides temperature variation of the TEG module under 5 W continues heat in Case#1 and Case#2.

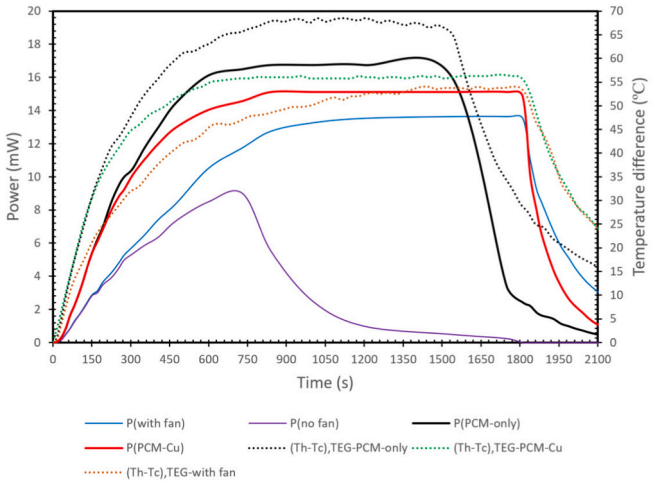

Fig. 5. Output power and hot sides temperature of the TEG systems under 5 W continues heat load.

(see Table 6) provided higher temperature difference and power generation in this case compared to the TEG in Case#1, where the maximum power generation was improved 11 % under continuous heat load of 5 W.

The copper foam makes opportunity to increase the heat load amplitude with safe operating temperature. Fig. 7 shows improvement of output power in the system with PCM-Cu versus the conventional TEG system operating with the cooling fan (Case#1). It took longer time to reach the critical temperature with the PCM-Cu heat sink. For instance, under continues heat load of 10 W, the TEG reached 150 °*C* after 488 s, 381 s and 705 s in the systems with the fan, PCM-only, and PCM—Cu, respectively. The temperature reduction on both sides of the TEG in the Case#4 with PCM-Cu was significant compared to the conventional system with the fan (Case#1). At the critical temperature, the cold side temperature of the TEG in Case #1 was at 79 °*C*, while the corresponding temperatures in the Case#4 were 25.3 % and 11.3 % lower, respectively.

Compared to the conventional TEG system with electrical fan, the system with the PCM-Cu enhanced the operating time, temperature difference across the TEG, and maximum power generation 44.4 %, 13.7 %, and 63.3 %, respectively. Results of the experiments show that, adding the metal foam not only is a useful tool to protect the system from overheating, but it also provides a suitable cooling technique more efficient than the conventional TEG system with electrical cooling fans. Another advantage of the proposed PCM-Cu based heat sink, introduced in this study, is a zero-cooling energy system with enhanced performance and net power.

4.3. Thermoelectric performance under periodic heat loads

To expand performance evaluation of the zero-cooling energy heat sink over types of heat loads, various heat loads with different amplitudes and durations (on/off time) were imposed to the hot side of the TEG. The temperature variation of the TEG under 5 W periodic heat load and with the on/off duration of 60 s and 240 s is shown in Fig. 8.

The hot side temperature of the fanless system in Case#2 quickly increased and reached the critical temperature after four thermal cycles due to the poor heat transfer coefficient on the surface of the heat sink exposed to the environment. The heat capacitance provided by the PCM compensated the low heat transfer coefficient in the fanless heat sink under periodic heat loads and kept the TEG systems under the critical temperature defined in this study. Lower hot and cold sides temperature of the TEG in the system with PCM-Cu in comparison with the PCM-only TEG system shows the significant effect of using the copper foam to reduce the thermal resistance from 4.65 ± 0.01 K/W to 0.98 K/W inside the PCM box. Unlike the continues heat loads, this improvement made higher temperature difference across the TEG system with the PCM-Cu compared to the system with PCM-only. For example, at 3600 s and

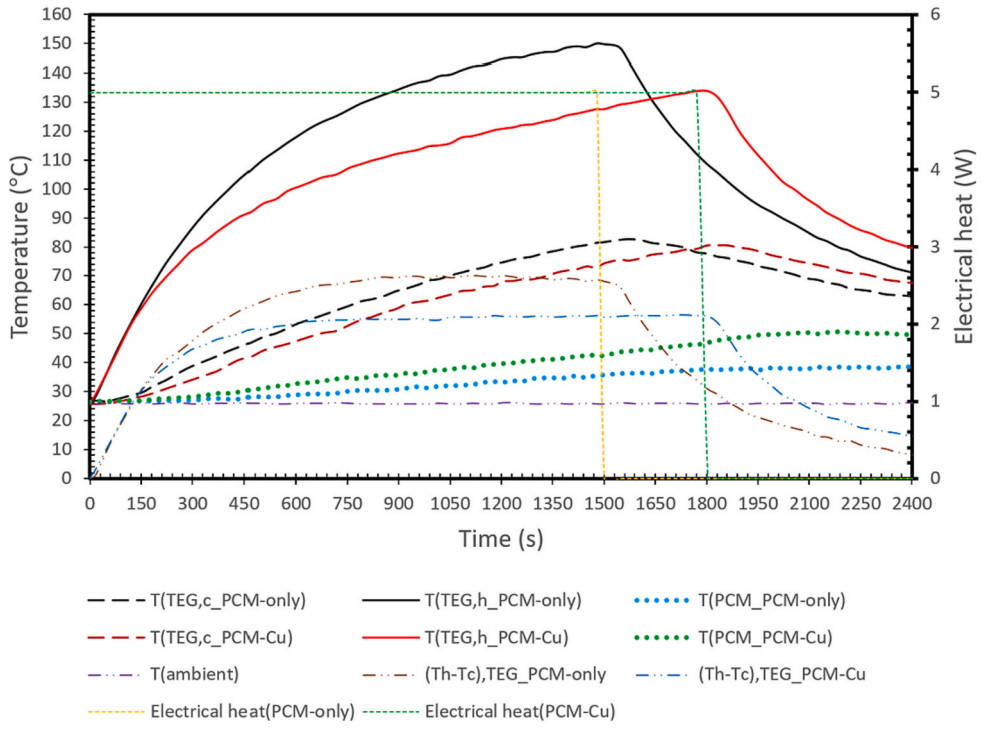

Fig. 6. Temperature difference and variation of TEG's hot and cold sides temperature, and imposed heat versus time in the systems with PCM-only and PCM-Cu heat sinks under continuous heat load of 5 W.

Table 8
Summary of mean value of voltage generation and standard deviation of voltage generation at 1800 s under 5 W heat load.

	Case#1	Case#2	Case#3	Case#4
Mean value of voltage generation (V)	0.3056	0.1256	0.2920	0.3713
Standard deviation (V)	0.1643	0.0725	0.1927	0.1748

under the heat load with the on/off duration of 60 s and 240 s, the temperature difference was improved 14 % and 19.3 %, respectively, by implementation of the metal foam in the PCM heat sink.

The PCM heat sink with lower thermal resistance enhanced thermal diffusion from the cold side of the TEG to the environmental ambient and increased the temperature difference across the TEG module causing higher output power under periodic heat loads. As shown in Fig. 9, although the minimum power output during the thermal cycles in the Case#3 and Case#4 are close to each other, there is a significant difference in the maximum output power. A main reason for such a difference is higher thermal diffusivity in the PCM heat sink integrated with the copper foam, which increases heat transfer rate inside the PCM. According to Tables 3 and 5, thermal diffusivity of the thermal storage material was enhanced 170 and 229 times inside the PCM-Cu heat sink (Case#4) compared to the PCM-only heat sink (Case#3) in the solid and fluid phases, respectively. Consequently, the maximum output power was increased 45.7 % in the TEG with the PCM-Cu heat sink.

Improvement of the thermal diffusivity in the thermal storage box made the TEG system with PCM-Cu capable of safe operating under higher heat fluxes. Consideration of the proposed systems under higher heat loads in Fig. 10 shows that, the hot side temperature stayed under the critical temperature in a longer time in the system with PCM-Cu heat sink compared to the system with PCM-only.

One of the beneficial impacts of the higher thermal diffusivity in the heat sink with PCM-Cu is increased rate of thermal storage in the PCM during the off duration. As result, in comparison with the PCM-only heat sink, this heat sink is more efficient to keep the system under the critical temperature at higher heat loads. For example, as shown in Fig. 10, increasing amplitude of the periodic heat load with on/off duration of 150s for 50 %, decreased the time to the critical temperature in the system with PCM-only heat sink 56.3 % while this reduction was 47.1 % in the system with PCM-Cu heat sink.

4.4. Energy harvesting improvement

Fig. 11 shows the energy harvested by the TEG in the systems studied in this work during the continues heating period from the initial condition until the overheating condition under heat loads of 5 W and 10 W. The TEG system with PCM-Cu heat sink produced the highest electrical energy amongst the studied systems. Although this improvement was comparable at lower heat loads, the energy production by the system with PCM-Cu heat sink was significantly higher compared to the other systems at the higher heat load. For instance, this system produced 311 %, 1.782 %, and 535 % higher energy compared with the systems in Case#1, Case#2, and Case#3, respectively, under the 10 W heat load. This result shows impact of integration of thermal energy storage materials and conductive metal foams forming an effective heat sink.

The results, furthermore, reveal that the system with PCM-only heat sink was not efficient as the conventional TEG system with electrical cooling fan in term of energy production. As Fig. 5 shows, although this system provided 18.3 % maximum output power higher than the system with cooling fan, it produced only 8.6 % higher electrical energy under heat load of 5 W. Under heat load of 10 W, this system generated only 58.2 % of the energy generated in the Case#1. The main reason for this decrement is the low thermal conductivity of the PCM, which anticipated the overheating condition. Therefore, to make a zero-cooling energy system but still efficient to prevent the TEG from the overheating condition, increasing thermal conductivity of the PCM heat sink via metal foams is necessary.

The energy harvesting improvement by the TEG system with PCM-Cu heat sink is also confirmed at periodic heat loads by results of Fig. 12. As discussed in Section 4.3, under the periodic heat loads this TEG system operates longer compared to the other cases before reaching the overheating temperature because of effective heat transfer to the PCM. As

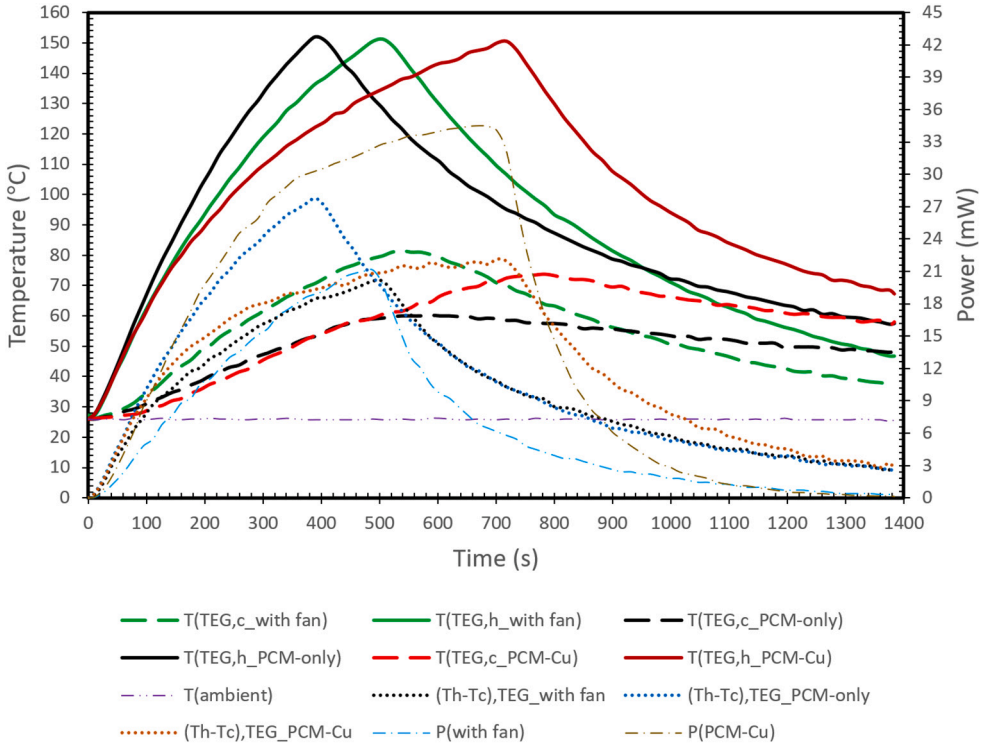

Fig. 7. Hot and cold sides temperature, temperature difference and output power of the TEG under continuous heat load of 10 W.

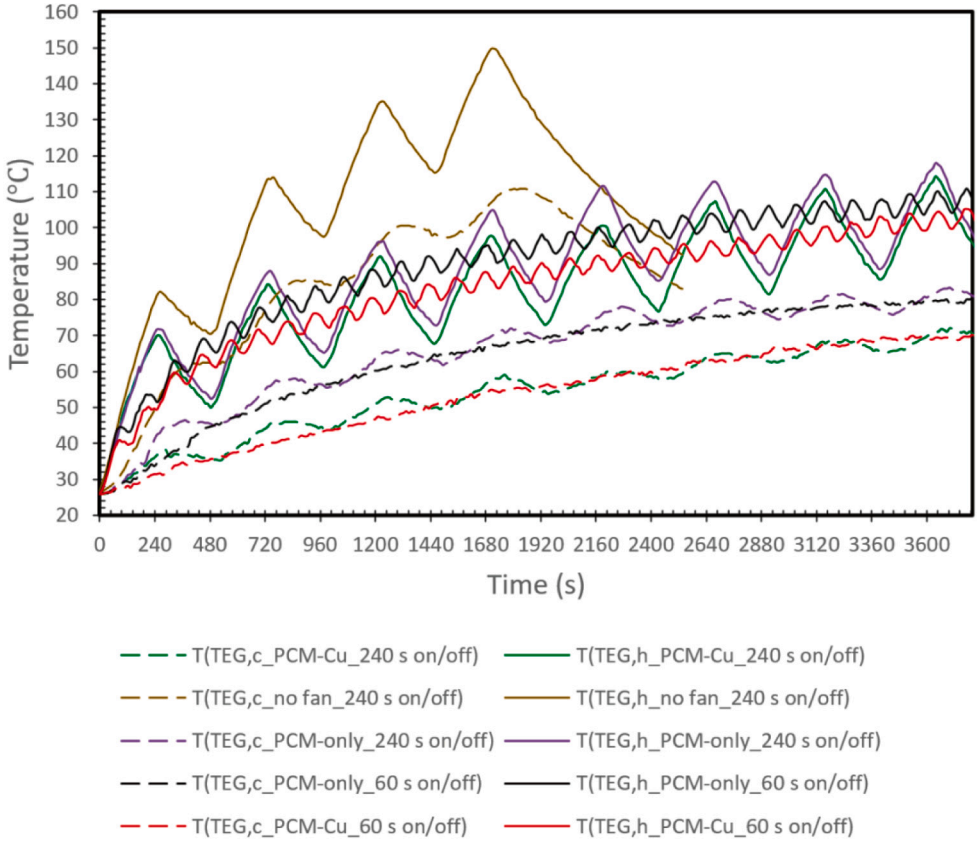

Fig. 8. Hot and cold sides temperature variation of the systems with zero-cooling energy heat sink under 5 W periodic heat load and with on/off duration of 60 s and 240 s.

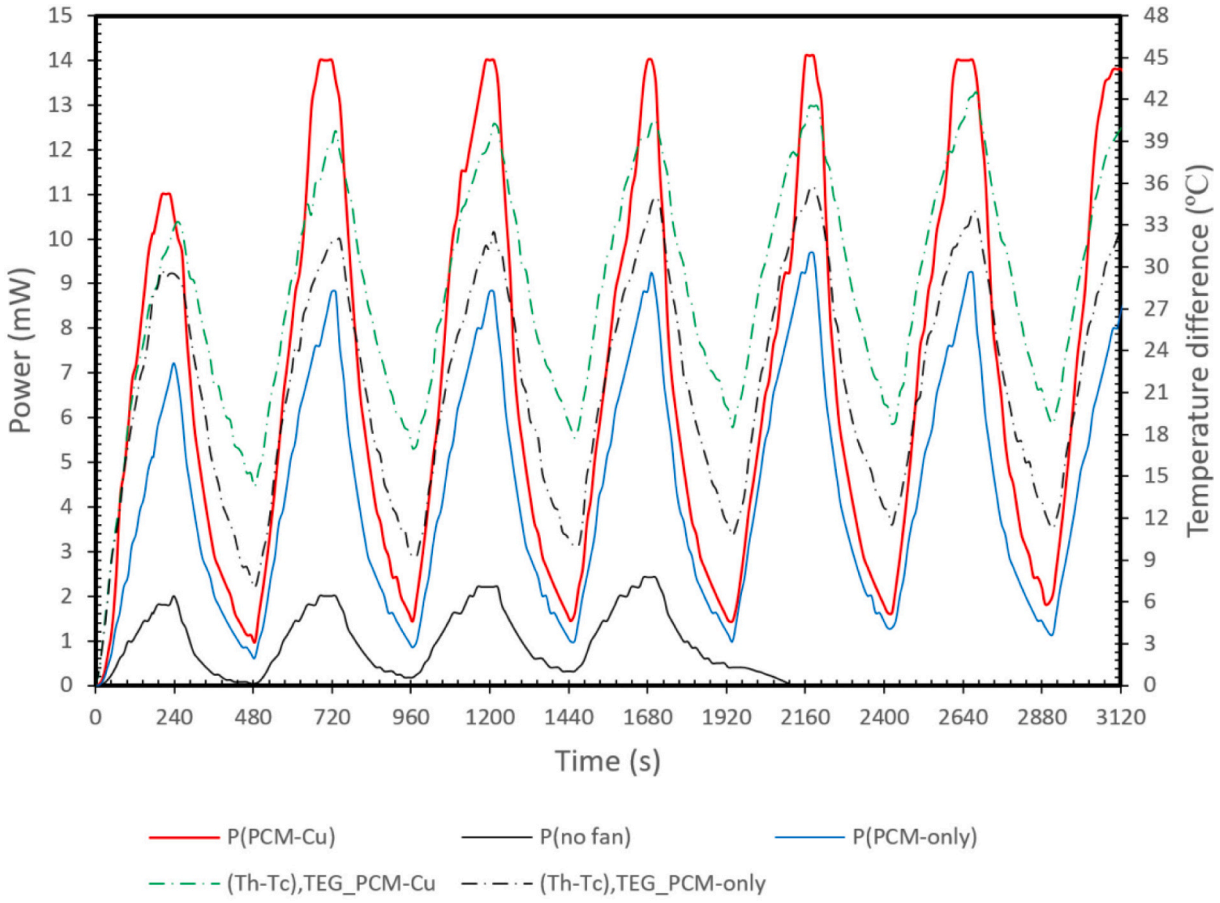

Fig. 9. Output power and temperature difference across the TEG under periodic heat load of 5 W with on/off duration of 240 s.

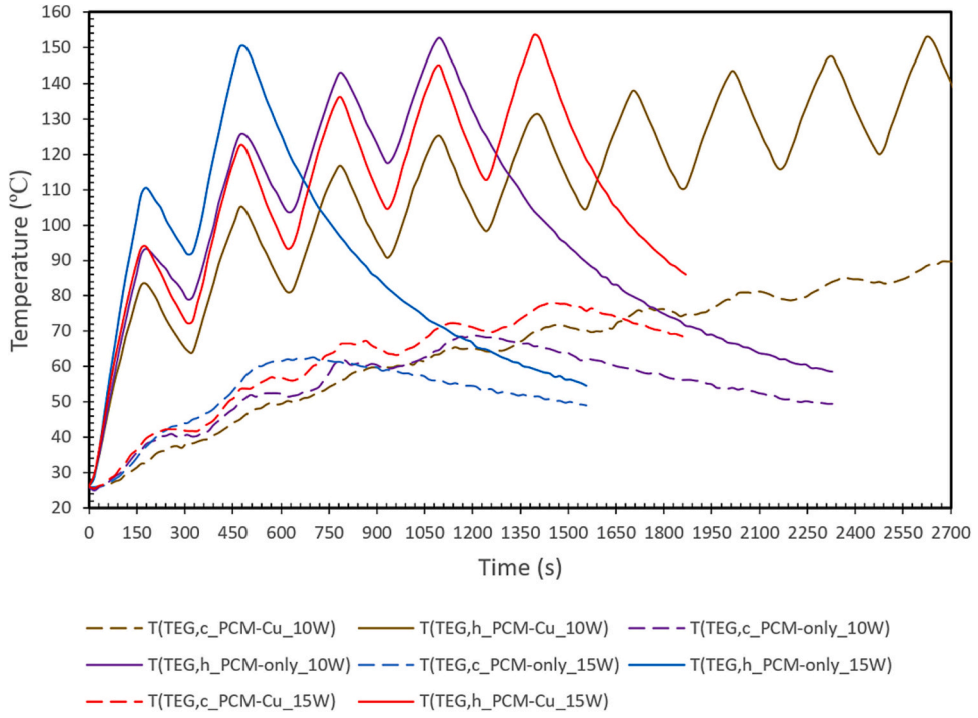

Fig. 10. Cold and hot sides temperature of the TEG under periodic heat loads of 10 W, 15 W with on/off duration of 150s in the systems with PCM-only and PCM—Cu.

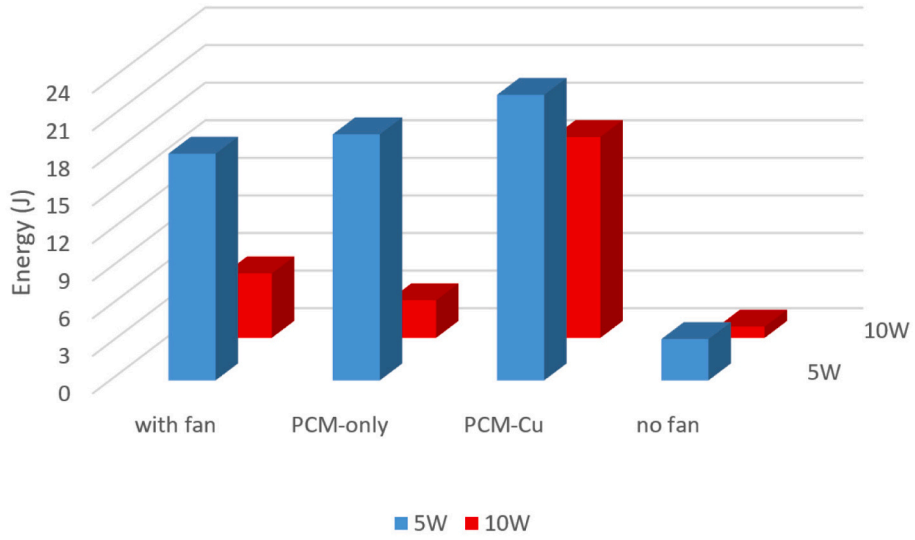

Fig. 11. Energy harvesting by the TEG under continues heat loads of 5 W and 10 W.

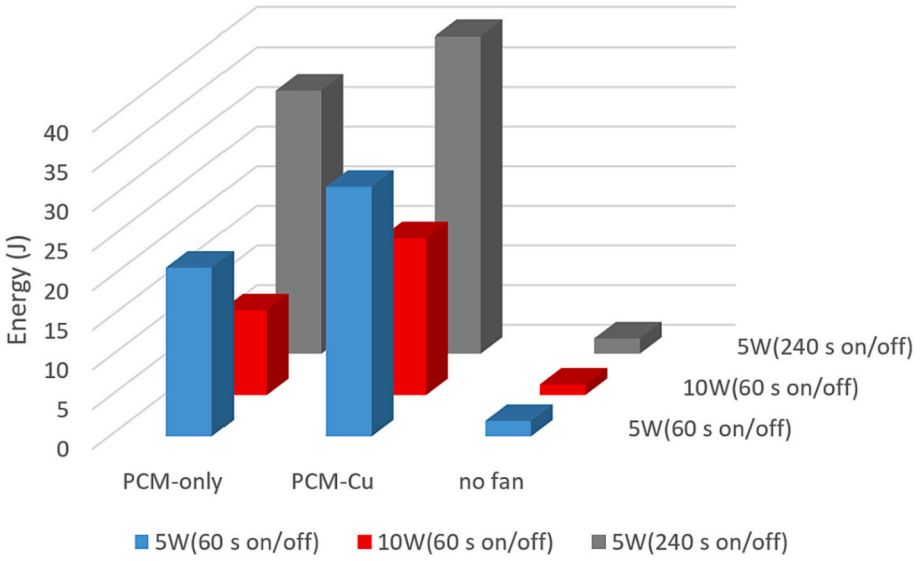

Fig. 12. Energy harvesting by TEG under periodic heat loads of 5 W and 10 W and on/off duration of 60 s and 240 s.

shown in Fig. 8, with the on/off duration of 240 s the PCM stored a fraction of the heat and prevented rapid increment of the TEG's cold side temperature. While the hot side temperature increased significantly, the higher temperature difference provided higher electrical power and energy. While the fanless TEG system in Case#2 did not have high energy harvesting performance, performance of the PCM-only system in term of energy generation was higher under periodic heat loads compared to the continues heat load conditions. Nevertheless, the TEG system with the PCM-Cu heat sink had best energy generation performance under periodic heat loads amongst systems evaluated in this study. For example, as Fig. 12 shows, applying the metal foam in the PCM box enhanced the energy generation 47.9 % and 85.4 % under heat loads of 5 W and 10 W, respectively, with on/off duration of 60 s.

As shown in Fig. 2, the volume of the modified cooling system with PCM is bigger than the standard cooling system with the cooling fan. This is a disadvantage of the cooling technology suggest in this study. However, the new concept makes the active cooling redundant and enhances reliability of thermoelectric systems. The results of this study, furthermore, indicate significant impact of integration of the copper metal foam with PCMs forming an effective energy storage module with enhanced thermal conductivity from the TEG to the environment ambient. Applying such fanless heat sink can improve economic saving in sensor and condition monitoring systems. With zero-cooling energy and maximizing net power production, autonomous thermoelectric energy harvesting systems can open a unique window of opportunity toward higher system efficiency in environmental [30] and industrial sensor [32] applications.

5. Conclusions

An experimental study was carried out to investigated feasibility of zero-cooling energy in thermoelectric systems operating under transient heat loads. In this study, PCM was integrated with copper metal foam on cold side of the TEG to explore impact of thermal conductivity of energy storage materials on temperature distribution in the thermoelectric system and output power of the TEG. Thus, temperature variations of the PCM at the middle of the storage box, the heat sink, and hot and cold sides of the TEG, as well as output voltage under optimal electrical load

were measured. Moreover, a compression on thermal-electrical response of the proposed TEG system is performed with conventional TEG system with fan, a fanless TEG system, and a TEG system with PCM heat sink but without the copper foam under dynamic heat loads with various intervals and continues heat loads imposed at ambient temperature.

Results of this study show that, applying cooper metal foam in the PCM box is a key factor to make a thermoelectric system with zero-cooling energy yet efficient under transient heat transfer conditions. Enhancement of thermal conductivity in this hybrid heat sink reduced the hot side temperature of the TEG and kept the TEG under the critical temperature at higher heat loads. The TEG system with PCM-Cu heat sink suggested in this study provided electric power generation higher than the conventional TEG system with electric cooling fan. In compression, the hot and cold sides temperature of the TEG decreased 25.3 % and 11.3 %, respectively, at continues heat load of 10 W, while the output power and energy generation increased up to 53.5 % and 85.4 % in the TEG system with the PCM-Cu heat sink. The results of this study offer a unique solution for feasibility of thermoelectric systems with zero-cooling energy under transient heat loads to reduce complexity of the system, while thermal and electrical responses of the system can be improved.

CRediT authorship contribution statement

Alireza Rezania: Conceptualization, Design of experiment, Methodology, Writing and editing original draft preparation, Investigation, Supervision.

Esmaeil Yousefi: Writing- Original draft preparation, Experimental setup, Experimental data, Data analysis, Visualization.

Ali Abbas Nejad: Methodology, Supervision, Investigation.

Declaration of competing interest

The authors declare that they have no known competing financial interests or personal relationships that could have appeared to influence the work reported in this paper.

Data availability

Data will be made available on request.

References

[1] J. Chen, et al., Enhanced efficiency of thermoelectric generator by optimizing mechanical and electrical structures, Energies 10 (9) (2017) 1329.
[2] S. Shittu, et al., Transient and non-uniform heat flux effect on solar thermoelectric generator with phase change material, Appl. Therm. Eng. 173 (2020), 115206.
[3] A. Goudarzi, et al., Integration of thermoelectric generators and wood stove to produce heat, hot water, and electrical power, J. Electron. Mater. 42 (7) (2013) 2127–2133.
[4] A. Rezania, L. Rosendahl, New configurations of micro plate-fin heat sink to reduce coolant pumping power, J. Electron. Mater. 41 (6) (2012) 1298–1304.
[5] D. Luo, et al., Modelling and simulation study of a converging thermoelectric generator for engine waste heat recovery, Appl. Therm. Eng. 153 (2019) 837–847.
[6] L.J. Zheng, H.W. Kang, A passive evaporative cooling heat sink method for enhancing low-grade waste heat recovery capacity of thermoelectric generators, Energy Convers. Manag. 251 (2022), 114931.
[7] S.A. Atouei, et al., Protection and thermal management of thermoelectric generator system using phase change materials: an experimental investigation, Energy 156 (2018) 311–318.
[8] Y. Tu, et al., A novel thermoelectric harvester based on high-performance phase change material for space application, Appl. Energy 206 (2017) 1194–1202.
[9] H.R. Abbasi, H. Pourrahmani, Multi-objective optimization and exergoeconomic analysis of a continuous solar-driven system with PCM for power, cooling and freshwater production, Energy Convers. Manag. 211 (2020), 112761.
[10] G. Lee, et al., Flexible heatsink based on a phase-change material for a wearable thermoelectric generator, Energy 179 (2019) 12–18.
[11] C. Selvam, et al., Enhanced thermal performance of a thermoelectric generator with phase change materials, Int. Commun. Heat Mass Transf. 114 (2020), 104561.
[12] S.A. Atouei, A.A. Ranjbar, A. Rezania, Experimental investigation of two-stage thermoelectric generator system integrated with phase change materials, Appl. Energy 208 (2017) 332–343.
[13] A. Rezania, S.A. Atouei, L. Rosendahl, Critical parameters in integration of thermoelectric generators and phase change materials by numerical and Taguchi methods, Mater. Today Energy 16 (2020), 100376.
[14] G. Muthu, et al., Performance of solar parabolic dish thermoelectric generator with PCM, Mater. Today: Proc. 37 (2021) 929–933.
[15] A. Bertacchini, S. Barbi, M. Montorsi, Improved heat sink for thermoelectric energy harvesting systems, in: International Conference on Intelligent Human Systems Integration, Springer, 2020.
[16] J. Yu, et al., A novel structure for heat transfer enhancement in phase change composite: rolled graphene film embedded in graphene foam, ACS Appl. Energy Mater. 2 (2) (2019) 1192–1198.
[17] X. Chenga, et al., Numerical study of forced convection over phase change material capsules in a traditional spherical shape and a biomimetic shape, J. Energy Storage 31 (2020), 101526.
[18] F. Wang, et al., Biomimetically calabash-inspired phase change material capsule: experimental and numerical analysis on thermal performance and flow characteristics, J. Energy Storage 52 (2022), 104859.
[19] Y. Dong, et al., N experimental and numerical study on flow characteristic and thermal performance of macro-capsules phase change material with biomimetic oval structure, Energy 238 (2022), 121830.
[20] W. Cui, et al., Heat transfer enhancement of phase change materials embedded with metal foam for thermal energy storage: a review, Renew. Sust. Energ. Rev. 169 (2022), 112912.
[21] H.M. Ali, Thermal performance analysis of metallic foam-based heat sinks embedded with RT-54HC paraffin: an experimental investigation for electronic cooling, J. Therm. Anal. Calorim. 140 (3) (2020) 979–990.
[22] E. Radomska, L. Mika, K. Sztekler, The impact of additives on the main properties of phase change materials, Energies 13 (12) (2020) 3064.
[23] J.R. Bose, et al., Comprehensive case study on heat transfer enhancement using micro pore metal foams: from solar collectors to thermo electric generator applications, Case Stud. Therm. Eng. 27 (2021), 101333.
[24] H.M. Ali, Heat transfer augmentation of porous media (metallic foam) and phase change material based heat sink with variable heat generations: an experimental evaluation, Sustain. Energy Technol. Assess. 52 (2022), 102218.
[25] E. Yousefi, et al., Higher power output in thermoelectric generator integrated with phase change material and metal foams under transient boundary condition, Energy 256 (2022), 124644.
[26] T. Wang, et al., Unidirectional thermal conduction in electrically insulating phase change composites for superior power output of thermoelectric generators, Compos. Sci. Technol. 225 (2022), 109500.
[27] S. Borhani, et al., Performance enhancement of a thermoelectric harvester with a PCM/metal foam composite, Renew. Energy 168 (2021) 1122–1140.
[28] K. Nithyanandam, R. Mahajan, Evaluation of metal foam based thermoelectric generators for automobile waste heat recovery, Int. J. Heat Mass Transf. 122 (2018) 877–883.
[29] S. Madruga, Thermoelectric energy harvesting in aircraft with porous phase change materials, in: IOP Conference Series: Earth and Environmental Science, IOP Publishing, 2019.
[30] S. Madruga, Modeling of enhanced micro-energy harvesting of thermal ambient fluctuations with metallic foams embedded in Phase Change Materials, Renew. Energy 168 (2021) 424–437.
[31] J. Duan, A novel heat sink for cooling concentrator photovoltaic system using PCM-porous system, Appl. Therm. Eng. 186 (2021), 116522.
[32] A. Mohammadnia, et al., Fan operating condition effect on performance of self-cooling thermoelectric generator system, Energy 224 (2021), 120177.
[33] C.H. Wan, et al., Design and experimental validation of an all-day passive thermoelectricsystem via radiative cooling and greenhouse effects, Energy 263 (2023), 125735.
[34] C.H. Wan, et al., Modelling and performance evaluation of a novel passive thermoelectric system based on radiative cooling and solar heating for 24-hour power-generation, Appl. Energy 331 (2023), 120425.
[35] A. Stupar, U. Drofenik, J.W. Kolar, Optimization of phase change material heat sinks for low duty cycle high peak load power supplies, IEEE Trans. Compon. Packag. Manuf. Technol. 2 (1) (2011) 102–115.
[36] S. Tiari, M. Mahdavi, Computational study of a latent heat thermal energy storage system enhanced by highly conductive metal foams and heat pipes, J. Therm. Anal. Calorim. 141 (5) (2020) 1741–1751.
[37] J.M. Mahdi, et al., Solidification enhancement with multiple PCMs, cascaded metal foam and nanoparticles in the shell-and-tube energy storage system, Appl. Energy 257 (2020), 113993.
[38] S. Weera, H. Lee, A. Attar, Utilizing effective material properties to validate the performance of thermoelectric cooler and generator modules, Energy Convers. Manag. 205 (2020), 112427.
[39] A. Rezania, E. Yazdanshenas, Effect of substrate layers on thermo-electric performance under transient heat loads, Energy Convers. Manag. 219 (2020), 113068.
[40] A. Rezania, L.A. Rosendahl, A comparison of micro-structured flat-plate and cross-cut heat sinks for thermoelectric generation application, Energy Convers. Manag. 101 (2015) 730–737.

[41] A. Allouhi, et al., Optimization of melting and solidification processes of PCM: application to integrated collector storage solar water heaters (ICSSWH), Sol. Energy 171 (2018) 562–570.

[42] W.-H. Chen, et al., A computational fluid dynamics (CFD) approach of thermoelectric generator (TEG) for power generation, Appl. Therm. Eng. 173 (2020), 115203.

[43] H.W. Coleman, W.G. Steele, Experimentation, Validation, And Uncertainty Analysis for Engineers, John Wiley & Sons, 2018.